Journal of ELECTRONIC MATERIALS, Vol. 43, No. 9, 2014
DOI: 10.1007/s11664-014-3187-1

Improving the Power Conversion Efficiency of Organic Solar Cell by Blending with CdSe/ZnS Core–Shell Quantum Dots

SHANG-CHOU CHANG,[1,3] YU-JEN HSIAO,[2] and TO-SING LI[1]

1.—Department of Electrical Engineering, Kun Shan University, Tainan City 71003, Taiwan. 2.—National Nano Device Laboratories, Tainan City 74147, Taiwan. 3.—e-mail: jchang@mail.ksu.edu.tw

We have blended poly(3-hexylthiophene) (P3HT) and [6,6]-phenyl C_{61} butyric acid methyl ester (PCBM) with CdSe/ZnS core–shell quantum dots (QDs) as the active layer to produce organic solar cells (OSC). The size of the CdSe/ZnS core–shell QDs was determined to be about 4 nm using transmission electron microscopy. The OSC were characterized by measuring the absorption spectra, current–voltage characteristics, and external quantum efficiency (EQE) spectra. The samples doped with 0.5 wt.% CdSe/ZnS core–shell QDs exhibited higher power conversion efficiency (PCE) than samples doped with other concentrations of QDs. The PCE of the OSC increases from 2.10% to 2.38% due to an increase of the short circuit current density (J_{sc}) from 6.00 mA/cm^2 to 6.25 mA/cm^2. The open circuit voltage (V_{oc}) was kept constant when comparing OSC that were undoped and doped with 0.5 wt.% CdSe/ZnS core–shell QDs. These CdSe/ZnS core–shell QDs can increase optical absorption as well as provide extra exciton dissociation and additional electric pathways in hybrid OSC.

Key words: P3HT, PCBM, CdSe/ZnS core–shell quantum dots, organic solar cells

INTRODUCTION

Using polymer materials is an attractive low-cost approach for fabricating photovoltaic devices. The bulk heterojunction solar cell is a promising one in organic solar cells (OSC). The active layer of bulk heterojunction solar cell is usually constructed by blending *p*-type conjugated polymers with *n*-type conjugated polymers, fullerenes, fullerene derivatives, or nanoparticles.[1–4]

Among numerous photoactive donor/acceptor composites, the *p*-type conjugated polymers with fullerene derivatives, like poly(3-hexylthiophene) (P3HT) and [6,6]-phenyl C_{61} butyric acid methyl ester (PCBM) blend, have been intensively investigated.[5,6] The OSC composed of π-conjugated polymers and fullerene derivatives have attracted considerable interest due to their lightness, simple solution processing, and bending capability.[7,8] Quantum dots (QDs), such as CdSe with high intrinsic charge carrier mobility, can also act as good electron acceptors, which are incorporated into *p*-type conjugated polymers like P3HT in OSC.[9]

The size of QDs is smaller than the exciton Bohr radius, leading to quantum confinement. Organic capping agents have often been added during synthesizing CdSe QDs for avoiding aggregation of nanoparticles. Greaney et al. applied the tert-butylthiol and Albero et al. applied the fullerene derivative C70 as the capping agent, respectively.[10,11]

Different capping agents bonded with CdSe QDs have been used for improving charge transport between donor and acceptor or among QDs in OSC. However, the low carrier mobility in QDs is often ascribed to inefficient charge transfer between QDs due to the presence of an organic capping agent.[11] The reported power conversion efficiency (PCE) of P3HT and CdSe QDs blend-based OSC is less than 2%.[9,11] Another way to prevent aggregation between CdSe QDs is to synthesize CdSe/ZnS core–shell QDs.[12] The large difference in bandgap between the

(Received October 7, 2013; accepted April 11, 2014; published online May 24, 2014)

CdSe core (1.74 eV) and the ZnS shell (3.61 eV) makes the excitons well confined to the core. The ZnS shell also passivates surface defects very well. The CdSe/ZnS core–shell QDs without a capping agent can be dispersed in OSC. Studies on adding the CdSe/ZnS core–shell QDs in silicon solar cells to improve PCE have been reported.[13] This work investigated the novel approach on CdSe/ZnS core–shell QDs incorporated in P3HT and PCBM blend (P3HT/PCBM)-based OSC. Light absorption was improved due to doping CdSe/ZnS core–shell QDs; therefore, an improvement in photovoltaic characteristics of OSC was expected. The absorption spectra, current–voltage and EQE characteristics of the P3HT/PCBM mixed with CdSe/ZnS core–shell QDs (P3HT/PCBM/CdSe/ZnS) were studied and discussed.

EXPERIMENTALS

The hybrid OSC were fabricated on indium tin oxide (ITO)-coated glass substrates. Patterned ITO substrates were oxygen plasma treated to increase hydrophilic property of the ITO surface. A layer of PEDOT:PSS about 40 nm thick was spin-coated on the ITO substrate and baked at 120°C for 30 min. The active layer consisted of P3HT (RMI-001E; Rieke Met., Lincoln, NE, USA) and PCBM ([60]PCBM; Nano-C, Westwood, MD, USA) in 10:8 wt.% ratio dissolved in 1,2-dichlorobenzene with various CdSe/ZnS core–shell QDs concentrations. The CdSe/ZnS core–shell QDs were dispersed in toluene.

The photoactive materials were spin-coated with a rotation speed of 800 rpm in a glove box, and the resulting film was about 300 nm thick. The P3HT/PCBM/CdSe/ZnS blended film was annealed at 120°C for 20 min to reduce the contact resistance of the electrodes. A Ca/Al electrode of 120 nm thickness was then deposited onto the active layer through a shadow mask by using thermal evaporation. The device structure of the produced OSC, in which P3HT/PCBM/CdSe/ZnS is the photoactive layer of the device, is shown in Fig. 1. The energy barrier is usually produced by charge accumulation at the interface between metal and PCBM in OSC. The short circuit current density (J_{sc}) and fill factor (FF) of OSC will increase after removing this energy barrier if Ca is selected as the metal cathode material.[14] The Al was deposited on top of the Ca as a protection layer due to the poor stability of Ca in air. The organic layer of anhydrous molecular residues must be controlled because Ca oxidizes when exposed to oxygen and moisture.[15] The device area was about 0.04 cm^2. The morphology of the CdSe/ZnS core–shell QDs was measured by a high-resolution transmission electron microscope (TEM). Then, the optical absorption spectra were obtained by using an optical spectrometer, and current–voltage measurements were obtained by using a source meter and a solar simulator with the AM 1.5 filter under an irradiation intensity of 100 mW cm^{-2}.

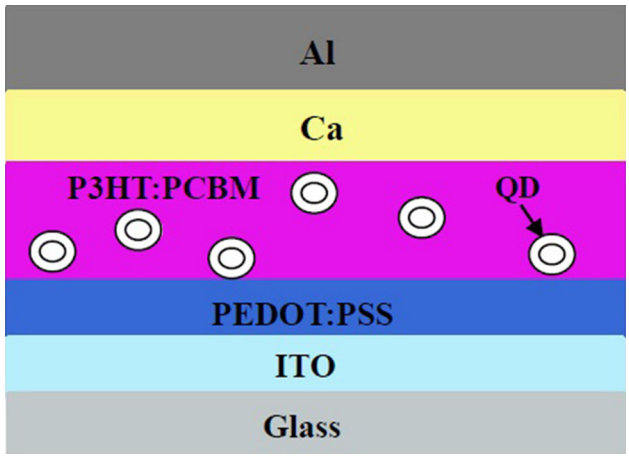

Fig. 1. The device structure of the P3HT/PCBM/CdSe/ZnS-based OSC.

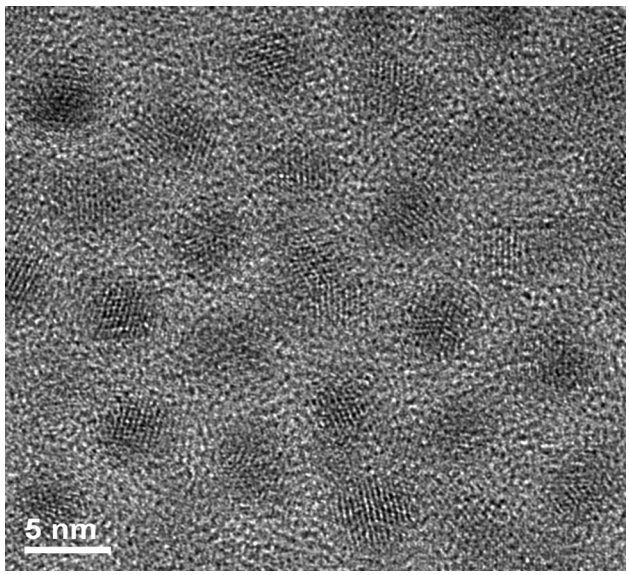

Fig. 2. TEM micrograph of CdSe/ZnS core–shell QDs.

RESULTS AND DISCUSSION

The TEM micrograph of the crystal CdSe/ZnS core–shell QDs shown in Fig. 2 provides further insight into the nanostructured properties. The spherical morphology is clearly observed from Fig. 2. The diameters of the QDs exhibit uniform dispersion and the average diameter is about 4 nm. Figure 3 presents the UV–Vis optical absorption spectra of the active layer with various concentrations of CdSe/ZnS core–shell QDs and also pure CdSe/ZnS core–shell QDs. The films prepared for optical absorption measurements were controlled with the same film thickness. The optical absorption apparently increases in the 300–700 nm wavelength region with significant growth in 300–400 nm, for QDs-doped active layer compared with that for pure P3HT/PCBM-based active layer

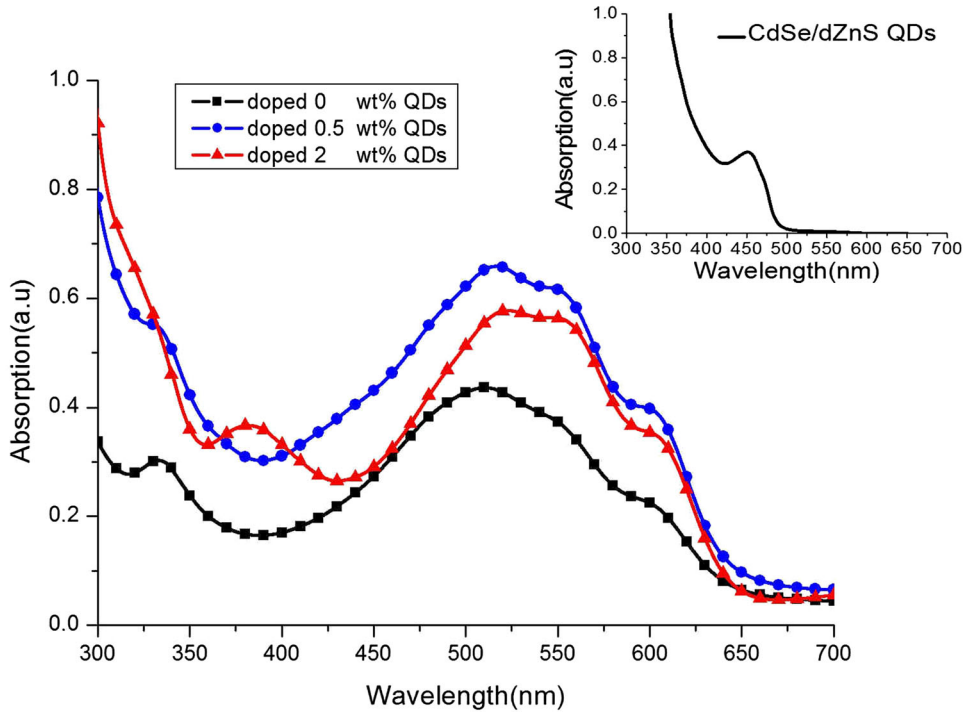

Fig. 3. Optical absorption spectra of P3HT/PCBM doped with various concentrations of CdSe/ZnS core–shell QDs.

obtained from Fig. 3. The pure CdSe/ZnS core–shell QDs-based active layer with respect to 300–400 nm region exhibits strong optical absorption as seen from the inset of Fig. 3. Mixing CdSe/ZnS core–shell QDs with P3HT/PCBM increases optical absorption of P3HT/PCBM-based active layer. In addition, the absorption peaks of various samples located at around 340 nm are attributed to the PCBM band, and those around 450–650 nm are attributed to the P3HT band in the optical absorption spectra.[16]

Figure 4 shows the corresponding electronic energy levels of P3HT, PCBM, and CdSe/ZnS core–shell QDs obtained from the reported literature.[16,17] The work function of CdSe/ZnS core–shell QDs is close to that of fullerenes. It provides the transport pathway of LUMO-fullerenes-CdSe/ZnS-Al leading to high electron mobility. Photo-generated electron–hole pairs can be dissociated at the interfaces between P3HT and CdSe/ZnS core–shell QDs. Consequently, extra energetically favorable pathways for the electrons transferring from the polymer to CdSe/ZnS core–shell QDs are introduced. Furthermore, photo-excited carriers generated in CdSe/ZnS core–shell QDs produce additional photocurrent as electrons and holes.

To study the effect of CdSe/ZnS core–shell QDs on device performance, the current density–voltage (J–V) characteristics of the produced OSC were measured under an illumination intensity of 100 mW/cm^2, shown in Fig. 5. The photovoltaic characteristics of samples doped with various concentrations of QDs are given in Table I. The results reveal that a low percentage of CdSe/ZnS core–shell QDs doping into the active layer produce an apparent increase in short circuit current density (J_{sc}) from 6.0 mA/cm^2 to 6.3 mA/cm^2, but the open circuit voltage (V_{oc}) remains the same for various doping concentrations including 0 wt.%. The PCE of the P3HT/PCBM/CdSe/ZnS-based OSC increases from 2.10% to 2.38%. They are higher than the reported PCE of P3HT and CdSe QDs blend-based OSC, which are smaller than 2%.[9,11]

The P3HT in the composite films gradually becomes an ordered structure (regioregularity) with suitable annealing. The PCE of solar cells therefore increases with annealing temperature up to 120°C. However, the aggregation of PCBM is due to high temperature annealing, resulting in phase separation and disruption of bi-continuous phases. This phenomenon increases the chance of short circuit and decreases the PCE in OSC.[18] Therefore, the best performance of OSC is made by 120°C annealing.

The samples doped with 0.5 wt.% CdSe/ZnS core–shell QDs exhibit higher PCE than other samples. The PCE and J_{sc} start to decrease when the concentrations of the CdSe/ZnS core–shell QDs exceed 0.5 wt.%. The CdSe/ZnS core–shell QDs function as the electron acceptors for P3HT/PCBM/CdSe/ZnS-based OSC. They can form common carrier transport networks which are accessible to PCBM.[19] The carrier mobility can therefore be improved,

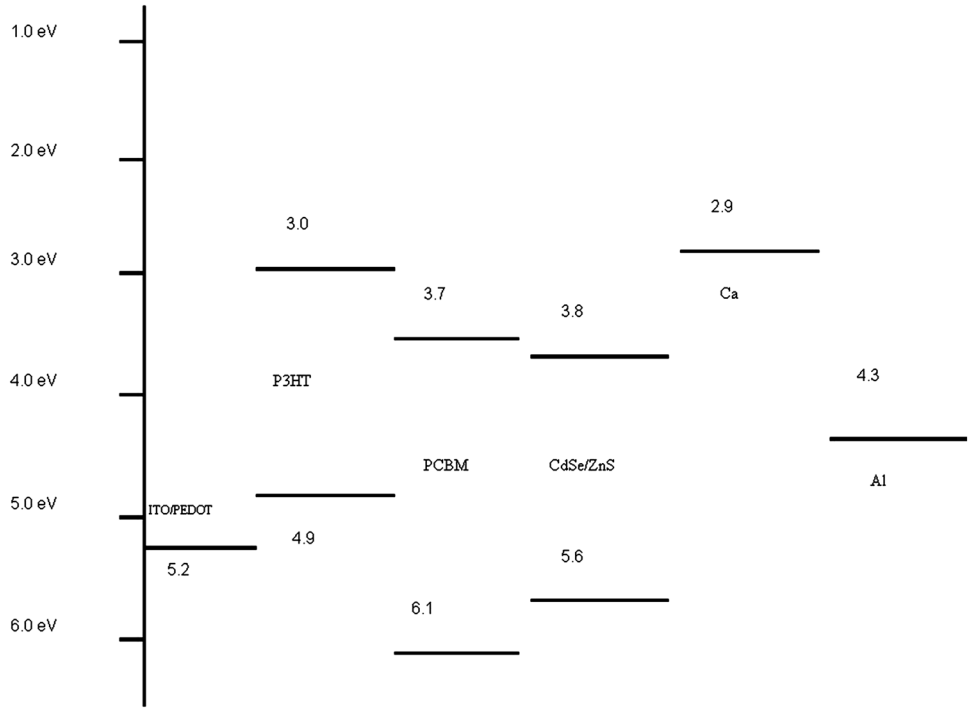

Fig. 4. Schematic energy level diagram of the P3HT/PCBM/CdSe/ZnS-based OSC.

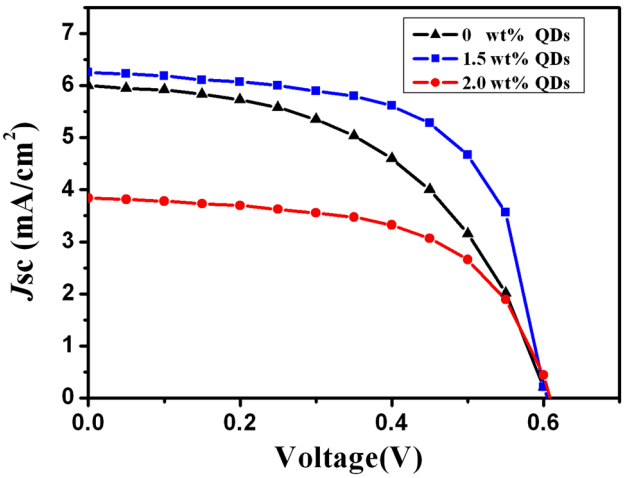

Fig. 5. *I–V* characteristics of OSC with various concentrations of CdSe/ZnS core–shell QDs.

resulting in an enhanced photocurrent of OSC. Moreover, incorporated CdSe/ZnS core–shell QDs is an
additional driving force for producing a higher fraction and larger sizes of PCBM clusters in the heterojunction structure.[20] Therefore, the resultant interconnecting PCBM clusters provide a better, more continuous pathway of charge carrier transport for P3HT/PCBM/CdSe/ZnS-based OSC compared with those for pure P3HT/PCBM-based OSC.

The samples doped with 0.5 wt.% CdSe/ZnS core–shell QDs exhibit higher PCE than other samples. Doping CdSe/ZnS core–shell QDs produces positive effects such as increasing interfaces between donors and acceptors, and optical absorption on photovoltaic performance. However, negative effects may also arise when QDs are doped into OSC. Doping nanoparticles into P3HT/PCBM-based OSC decreases the performance of OSC due to quenching of the excited state in the polymer. Segregation phenomena in OSC have been reported.[21] The scenario may be related to why the PCE and J_{sc} starts to decrease when the concentration of CdSe/ZnS core–shell QDs exceeds 0.5 wt.%. Further interpretations on this will be explored.

The FF corresponding to 2 wt.% QDs is lower than that corresponding to 0.5 wt.% QDs shown in Table I. This result indicates that the shunt resistance of the OSC is relatively low, implying that leakage current occurs in the OSC.[22]

External quantum efficiency (EQE) spectra for the P3HT/PCBM and P3HT/PCBM/CdSe/ZnS OSC are displayed in Fig. 6. All EQE spectra are similar in shape, while the EQE values of samples containing 0.5 wt.% QDs doping are higher than other samples. For example, the OSC of P3HT/PCBM were found to have the EQE maximum of 40.8% located at 490 nm, whereas the EQE of the OSC with 0.5 wt.% QDs doping is 42.4% at the same wavelength. These CdSe/ZnS core–shell QDs can increase optical absorption, as well as provide extra exciton dissociation and additional electric pathways in the active layer of OSC, thereby enhancing J_{sc}.

Table I. Photovoltaic performance of OSC with various concentrations of CdSe/ZnS core–shell QDs, under AM1.5G at 100 mW/cm^2 illumination

Doping concentration (wt.%)	V_{oc} (V)	J_{sc} (mA/cm^2)	FF	PCE (%)
0	0.599 ± 0.01	6.00 ± 0 17	58.56 ± 0.97	2.10 ± 0 08
0.2	0.599 ± 0.01	6.05 ± 0.21	60.97 ± 1.02	2.21 ± 0.11
0.5	0.599 ± 0.01	6.25 ± 0.20	63.33 ± 0.95	2.38 ± 0.11
1.2	0.599 ± 0.01	5.28 ± 0.18	59.59 ± 1.03	1.88 ± 0.09
2.0	0.599 ± 0.01	3.84 ± 0.15	59.92 ± 1.06	1.38 ± 0.08

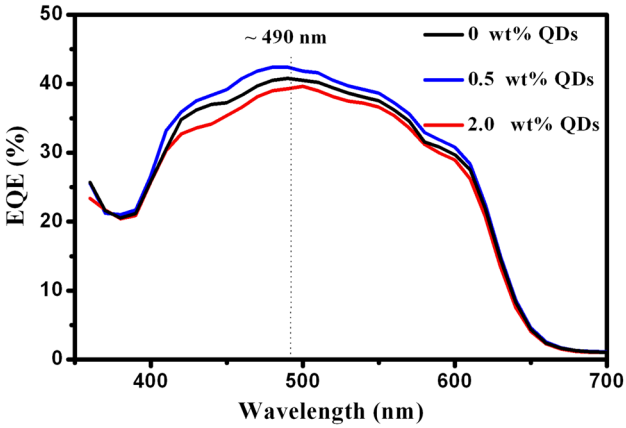

Fig. 6. EQE spectra of OSC with various concentrations of CdSe/ZnS core–shell QDs.

CONCLUSIONS

We have made OSC by blending P3HT/PCBM with CdSe/ZnS core–shell QDs. The size of the crystalline CdSe/ZnS core–shell QDs observed using TEM was about 4 nm. The samples doped with 0.5 wt.% CdSe/ZnS core–shell QDs demonstrate higher PCE than other samples. The PCE of the devices increases from 2.1% to 2.4%, resulting in an increase of J_{sc} from 6.0 mA/cm^2 to 6.3 mA/cm^2. These CdSe/ZnS core–shell QDs can increase optical absorption, as well as provide extra exciton dissociation and additional electrical pathways in hybrid OSC.

ACKNOWLEDGEMENT

The authors would like to thank the National Science Council of Taiwan for financially supporting this research under Grant NSC 102-2221-E-168-037.

REFERENCES

1. S. Gunes, H. Neugebauer, and N.S. Sariciftci, *Chem. Rev.* 107, 1324 (2007).
2. P.V. Kamat, *J. Phys. Chem. C* 111, 2834 (2007).
3. P.V. Kamat, *J. Phys. Chem. C* 112, 18737 (2008).
4. B.R. Saunders and M.L. Turner, *Adv. Colloid Interface Sci.* 138, 1 (2008).
5. S.W. Lee, H.J. Lee, J.H. Choi, W.G. Koh, J.M. Myoung, J.H. Hur, J.J. Park, J.H. Cho, and U. Jeong, *Nano Lett.* 10, 347 (2010).
6. G. Li, V. Shrotriya, J.S. Huang, Y. Yao, T. Moriarty, K. Emery, and Y. Yang, *Nat. Mater.* 4, 864 (2005).
7. T.F. Guo, T.C. Wen, G.L. Pakhomov, X.G. Chin, S.H. Liou, and P.H. Yeh, *Thin Solid Films* 516, 3138 (2008).
8. F.C. Chen, J.L. Wu, C.L. Lee, W.C. Huang, H.M. Chen, and W.C. Chen, *IEEE Electron. Dev. Lett.* 30, 727 (2009).
9. Y. Zhou, F.S. Riehle, Y. Yuan, H. Schleiermacher, M. Niggemann, G.A. Urban, and M. Krüger, *Appl. Phys. Lett.* 96, 013304 (2010).
10. M.J. Greaney, S. Das, D.H. Webber, S.E. Bradforth, and R.L. Brutchey, *ACSNANO* 6, 4222 (2012).
11. J. Albero, P. Riente, J.N. Clifford, M.A. Pericàs, and E. Palomares, *J. Phys. Chem. C* 117, 13374 (2013).
12. B.O. Dabbousi, J. Rodriguez-Viejo, F.V. Mikulec, J.R. Heine, H. Mattoussi, R. Ober, K.F. Jensen, and M.G. Bawendi, *J. Phys. Chem. B* 101, 9463 (1997).
13. A.M. Suhail, G.S. Muhammed, A.N. Naje, R.R. Mohammed, and H.I. Murad, *Int. J. Sci. Adv. Technol.* 2, 133 (2012).
14. J. Xue, B.P. Rand, and S.R. Forrest, *Org. Photovolt. VII* 6334, 63340K (2006).
15. B. Paci, A. Generosi, V.R. Albertini, P. Perfetti, R. de Bettignies, and C. Sentein, *Chem. Phys. Lett.* 461, 77 (2008).
16. C.W. Liang, W.F. Su, and L. Wang, *Appl. Phys. Lett.* 95, 133303 (2009).
17. Q. Shen, J. Kobayashi, L.J. Diguna, and T. Toyoda, *J. Appl. Phys.* 103, 84304 (2008).
18. Y.-C. Huang, Y.-C. Liao, S.-S. Li, M.-C. Wu, C.-W. Chen, and W.-F. Su, *Solar Energy Mater Solar Cells* 93, 888 (2009).
19. S.K. Dixit, S. Madan, D. Madhwal, J. Kumar, I. Singh, C.S. Bhatia, P.K. Bhatnagar, and P.C. Mathur, *Org. Electron.* 13, 710 (2012).
20. H.C. Liao, C.S. Tsao, T.H. Lin, M.H. Jao, C.M. Chuang, S.Y. Chang, Y.C. Huang, Y.T. Shao, C.Y. Chen, C.J. Su, U.S. Jeng, Y.F. Chen, and W.F. Su, *ACS Nano* 6, 1657 (2012).
21. K. Topp, H. Borchert, F. Johnen, A.V. Tunc, M. Knipper, E.V. Hauff, J. Parisi, and K. Al-Shamery, *J. Phys. Chem. A* 114, 3981 (2010).
22. M.S. Kim, B.G. Kim, and J. Kim, *ACS Appl. Mater. Interfaces* 1, 1264 (2009).